Article

Closed-form Expressions of Generalized Conforming Triangular Finite Element for Thermal Bending Analysis of Thin Plate

Chatthanon Bhothikhun

Department of Mechanical Engineering, Faculty of Engineering and Industrial Technology, Silpakorn University, Nakhon Pathom, Thailand, 73000
E-mail: chatthanon@outlook.com (Corresponding author)

Abstract. The generalized conforming triangular finite element for thermal bending analysis of thin plate caused by the temperature difference along the plate thickness is developed. The finite element formulation with detailed finite element matrices is derived based on the modified potential energy principle and the generalized compatibility conditions. The closed-form expressions of the stiffness matrix and the thermal loading which can be applied directly to the computer program are also derived and presented. The performance of the generalized conforming triangular element is evaluated by several examples of which the exact solutions are known. The results demonstrate that the generalized conforming triangular element performs very well for thermal bending analysis of thin plate.

Keywords: Thermal bending, thin plate, generalized conforming element.

This article is based on the presentation at the International Conference on Engineering and Industrial Technology (ICEIT 2020) in Chonburi, Thailand, 11th-13th September 2020.

1. Introduction

The finite element method has been widely used in plate bending analysis as the exact solutions of the real applications are difficult to be found. One of the difficulties of the finite element in plate bending analysis is the requirement of C_1 continuity. As a result of this necessity, the value of transverse deflection, w, and its slope must impose continuity between adjacent elements. Such difficulties contribute to several types of plate bending elements which have been developed during the past decades [1-4].

Early developed plate bending elements in finite element analysis were the non-conforming element, such as the well-known BCIZ triangular element [5]. The BCIZ element provided reliable solution accuracy in plate bending analysis. The element was named non-conforming element because the normal slope along the element edges cannot be represented by the corner node connections. In addition, it was found that the solution obtained from the non-conforming elements sometimes was superior to that obtained from the conforming element type. However, these non-conforming plate bending elements sometimes conduced to divergent results in some problems so that the convergence to the accurate result from this element type could not be ensured. Meanwhile, the conforming element types were complicated to formulate and were too stiff as it imposed undue conditions of continuity [6]. As a result, the conforming elements generally did not used in the real applications. Another element type was the DKT element which derived by discrete Kirchhoff theory [3]. Even though this element provided accurate solution [7, 8], the element formulation was quite complicated and the transverse displacement was defined only along element sides.

Another type of thin plate bending element was the generalized conforming element [9]. The element was formulated based on the modified potential energy principle and the generalized compatibility conditions with the compatibility conditions at nodes and along the sides of the element [10]. The nine degrees of freedom generalized conforming triangular element then can be formulated. The result obtained from the element passed the patch test and provided accurate results. The generalized conforming element was also easy to program as the closed-form expression of the corresponding finite element matrices can be derived explicitly. However, the finite element formulations of this element were derived only for plate bending analysis under the applied transverse mechanical loading. The finite element matrices of this element in thermal plate bending analysis has not been found in any literature. The main objective of this study is to present the finite element formulation and the performance of the generalized conforming triangular element in thin plate bending analysis under thermal loading.

The paper begins with the corresponding governing partial differential equations of the thin plate bending.

The closed-form expressions of finite element equations that include the proposed finite element matrices according to thermal plate bending. Then, the proposed thermal load vector is derived and presented. Finally, some thin-plate thermal bending problems with exact solutions are used to evaluate the performance of the proposed finite element formulations. Such solutions are also compared with the solutions obtained from the well-known nonconforming triangular thin plate bending element (BCIZ) and the discrete Kirchhoff triangular element (DKT).

2. Governing Equations

The governing equation of thin plate bending problems with the transverse deflection w in the z-direction normal to the x-y plane of thin plate and the temperature distribution $T(z)$ along the plate thickness t is given by [11],

$$
D\left(\frac{\partial^4 w}{\partial x^4} + 2\frac{\partial^4 w}{\partial x^2 \partial y^2} + \frac{\partial^4 w}{\partial y^4}\right) = \\
-\frac{1}{1-\nu}\left(\frac{\partial^2 M_T}{\partial x^2} + \frac{\partial^2 M_T}{\partial y^2}\right) + p(x, y)
\tag{1}
$$

where $p(x,y)$ is the applied transverse mechanical load normal to the x-y plane, ν is Poisson's ratio and D is the bending rigidity which can be defined as,

$$
D = \frac{Et^3}{12(1-\nu^2)}
\tag{2}
$$

where t is the thickness of the plate and E is the mod ulus of elasticity. The thermal moment M_T in Eq. (1) is defined by,

$$
M_T = E\alpha \int_{-t/2}^{t/2} (T(z) - T_0)z \, dz
\tag{3}
$$

where α is thermal expansion coefficient.

3. Finite Element Equations

The modified potential energy theorem was used to derive the generalized conforming triangular plate bending finite element formulations as [12],

$$
\Pi_{mp} = \Pi_p - \sum H = \text{stationary}
\tag{4}
$$

$$
\Pi_p = \iint_{A_e} \frac{D}{2}\left[\left(\frac{\partial^2 w}{\partial x^2}\right)^2 + \left(\frac{\partial^2 w}{\partial y^2}\right)^2 + 2\nu\frac{\partial^2 w}{\partial x^2}\frac{\partial^2 w}{\partial y^2} \right. \\
\left. + 2(1-\nu)\left(\frac{\partial^2 w}{\partial x \partial y}\right)^2\right] dx \, dy - \iint_{A_e} p \, w \, dx \, dy
\tag{5}
$$

$$H = \int_{\partial A_e} \left[M_n \left(\frac{\partial w}{\partial n} + \tilde{\theta}_s \right) + M_{ns} \left(\frac{\partial w}{\partial s} - \frac{\partial \tilde{w}}{\partial s} \right) - Q_n \left(w - \tilde{w} \right) \right] ds \quad (6)$$

where Π_p and Π_{mp} are functions of minimum and modified potential energy theorems, respectively. H is the additional energy corresponding to the displacements on the element side ∂A_e in which Q_n, M_n and M_{ns} are Lagrange multipliers which represent the transverse shear, normal moment and twisting moment on the boundary ∂A_e, n and s represent the normal and tangential directions of the element side, respectively. w is the transverse deflection inside the element. $\tilde{w}$ is the deflection along the side of the element. And $\tilde{\theta}_s$ is the rotation about the tangential axis s on ∂A_e.

With the limit size of the element that tends to zero, the additional energy H in Eq. (6) becomes,

$$H = \int_{\partial A_e} \left[M_n \left(\frac{\partial w}{\partial n} + \tilde{\theta}_s \right) + M_{ns} \left(\frac{\partial w}{\partial s} - \frac{\partial \tilde{w}}{\partial s} \right) - Q_n \left(w - \tilde{w} \right) \right] ds = 0 \quad (7)$$

Therefore, Π_{mp} degenerates to Π_p. The element stiffness matrix then can be derived based on the Π_p.

We then firstly apply the integration by parts and rewrite Eq. (7) as,

$$H = \int_{\partial A_e} \left[M_n \left(\frac{\partial w}{\partial n} + \tilde{\theta}_s \right) - \left(Q_n + \frac{\partial M_{ns}}{\partial s} \right) \left(w - \tilde{w} \right) \right] ds$$
$$+ \sum_j \left(\Delta M_{ns} \right)_j \left(w - \tilde{w} \right)_j \quad = \quad 0 \quad (8)$$

where j represents the nodal point of the element and $\left(\Delta M_{ns} \right)_j$ is the difference between the twisting moments acting at the sides connected with nodal point j. Therefore, the deflection field w is assumed to meet the congruent conditions as,

$$\left(w - \tilde{w} \right)_j = 0 \quad \text{(at each node } j \text{)} \quad (9)$$

$$\int_{S_k} \left(w - \tilde{w} \right) ds = 0 \quad (10)$$

$$\int_{S_k} \left(\frac{\partial w}{\partial n} + \tilde{\theta}_s \right) ds = 0 \quad \text{(on each side } S_k \text{)} \quad (11)$$

Equation (9) is the point compatibility condition and Eqs. (10)-(11), are the line compatibility conditions at nodes and along the sides of the element.

A triangular element with nine degrees of freedom (DOF) is shown in Fig. 1. The vector of nodal unknowns $\{\delta\}^e$ is defined as,

$$\{\delta\}^e = \lfloor w_1 \quad \theta_{x1} \quad \theta_{y1} \quad w_2 \quad \theta_{x2} \quad \theta_{y2} \quad w_3 \quad \theta_{x3} \quad \theta_{y3} \rfloor^T \quad (12)$$

where $\theta_{xi} = \left(\partial w / \partial y \right)_i$ and $\theta_{yi} = -\left(\partial w / \partial x \right)_i$ denote the nodal rotations.
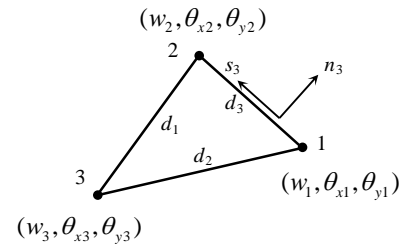

Fig. 1. Triangular plate bending element with 9 DOF.

The deflection $\tilde{w}$ and normal slope $\tilde{\theta}_s$ along the element side 12 are supposed to be cubic and linear distribution respectively as,

$$\tilde{w}_{12} = \left(L_1 + L_1^2 L_2 - L_2^2 L_1 \right) w_1 - b_3 L_1^2 L_2 \theta_{x1} - c_3 L_1^2 L_2 \theta_{y1}$$
$$+ \left(L_2 + L_2^2 L_1 - L_1^2 L_2 \right) w_2 + b_3 L_2^2 L_1 \theta_{x2} + c_3 L_2^2 L_1 \theta_{y2} \quad (13)$$

$$\tilde{\theta}_{s12} = \frac{1}{d_3} \left[L_1 \left(c_3 \theta_{x1} - b_3 \theta_{y1} \right) + L_2 \left(c_3 \theta_{x2} - b_3 \theta_{y2} \right) \right] \quad (14)$$

where L_i (i = 1, 2, 3) represents area coordinates [11], d_i (i = 1, 2, 3) represents the length of the element side, and $b_3 = y_1 - y_2$ and $c_3 = x_2 - x_1$ are the coefficients appear in the area coordinates. Analogous expressions for the side 23 and 31 of the element can be derived by permutation.

Therefore, the deflection field w over the element can be express as,

$$w = w_1 L_1 + w_2 L_2 + w_3 L_3 + \hat{w} \quad (15)$$

and

$$\hat{w} = \lambda_1 L_1 L_2 + \lambda_2 L_2 L_3 + \lambda_3 L_3 L_1 + \lambda_4 F_4 + \lambda_5 F_5 + \lambda_6 F_6 \quad (16)$$

where

$$F_4 = L_1 \left(L_1 - 1/2 \right) \left(L_1 - 1 \right)$$
$$F_5 = L_2 \left(L_2 - 1/2 \right) \left(L_2 - 1 \right) \quad (17)$$
$$F_6 = L_3 \left(L_3 - 1/2 \right) \left(L_3 - 1 \right)$$

The nodal compatibility condition Eq. (9) is then already satisfied. The coefficients λ_1, λ_2, ..., λ_6 in Eq. (16) can be obtained from Eqs. (10) and (11).

Consequently, the deflection field w can be rewritten in matrices as,

$$w = \lfloor N \rfloor \{\delta\}^e = \sum_{i=1}^3 \left(N_i w_i + N_{xi} \theta_{xi} + N_{yi} \theta_{yi} \right) \quad (18)$$

where

$$N_1 = L_1 - 2F_4 + (1 - r_2)F_5 + (1 + r_3)F_6$$
$$N_{x1} = -\frac{b_3}{2} L_1 L_2 + \frac{b_2}{2} L_3 L_1 - \frac{1}{2}(b_2 - b_3)F_4$$

$$-\frac{1}{2}(r_2 b_2 + b_3)F_5 - \frac{1}{2}(r_3 b_3 - b_2)F_6 \qquad (19)$$

$$N_{y1} = -\frac{c_3}{2}L_1 L_2 + \frac{c_2}{2}L_3 L_1 - \frac{1}{2}(c_2 - c_3)F_4$$
$$-\frac{1}{2}(r_2 c_2 + c_3)F_5 - \frac{1}{2}(r_3 c_3 - c_2)F_6$$

and

$$r_1 = \frac{d_2{}^2 - d_3{}^2}{d_1{}^2}, \quad r_2 = \frac{d_3{}^2 - d_1{}^2}{d_2{}^2}, \quad r_3 = \frac{d_1{}^2 - d_2{}^2}{d_3{}^2} \qquad (20)$$

The expression for six other shape functions (N_2, N_{x2}, N_{y2}, N_3, N_{x3} and N_{y3}) can be derived by permutation. According to these element shape functions, the element stiffness matrix $[K]$ can then be derived.

The finite element equations for thermal bending analysis of thin plate can then be written as,

$$[K]\{\delta\} = \{F_T\} + \{F_p\} \qquad (21)$$

where $[K]$ is the element stiffness matrix, $\{\delta\}$ is the vector of the element nodal unknowns which contains transverse deflection and the rotations at each node as in Eq. (12), and $\{F_T\}$ is the nodal thermal load associated with the temperature gradient through the plate thickness. While $\{F_p\}$ is the nodal force vector due to the applied lateral loads which is not considered in this study.

The element stiffness matrix $[K]$ of the generalized conforming triangular element is given by,

$$[K] = \iint_A [B]^T [D][B]\,dA \qquad (22)$$

where

$$[D] = \frac{Et^3}{12(1-v^2)}\begin{bmatrix} 1 & v & 0 \\ v & 1 & 0 \\ 0 & 0 & \dfrac{1-v}{2} \end{bmatrix} \qquad (23)$$

and

$$[B] = \begin{bmatrix} -\left\lfloor \dfrac{\partial^2 N}{\partial x^2} \right\rfloor \\ -\left\lfloor \dfrac{\partial^2 N}{\partial y^2} \right\rfloor \\ -2\left\lfloor \dfrac{\partial^2 N}{\partial x \partial y} \right\rfloor \end{bmatrix} \qquad (24)$$

The closed form expression of the stiffness matrix can be rewritten as follows,

$$[K] = [R]^T [Q][R] \qquad (25)$$

where the matrices $[R]$ and $[Q]$ is given in Appendix.

The vector of the nodal forces due to the thermal load $\{F_T\}$ in Eq. (21) can be defined as,

$$\{F_T\} = \frac{1}{1-v}\int_A [B]^T \{M\}\,dA \qquad (26)$$

where the vector $\{M\}$ is given by,

$$\{M\}^T = \lfloor M_T \quad M_T \quad 0 \rfloor \qquad (27)$$

The thermal moment, M_T is defined as in Eq. (3). The vector of the nodal forces due to the thermal load $\{F_T\}$ in Eq. (26) can be rewritten as,

$$\{F_T\} = \frac{1}{1-v}M_T \int_A [B]^T\,dx\,dy \begin{Bmatrix} 1 \\ 1 \\ 0 \end{Bmatrix} \qquad (28)$$

or $\qquad \{F_T\} = \dfrac{1}{1-v}M_T[BA]\begin{Bmatrix} 1 \\ 1 \\ 0 \end{Bmatrix} \qquad (29)$

where the closed form expression of matrix $[BA]$ is shown in Appendix.

The closed-form expressions of the thermal load vector in Eq. (29) which have been derived firstly in this study can be applied in the computer programming directly. The performance of the proposed thermal load vector above is then examined by thermal plate bending examples of which exact solutions are existed in the next section.

4. Applications

Three examples are used to evaluate the performance of the generalized conforming triangular (GCT) plate bending element with the proposed closed form finite element formulations.

4.1. Simply Supported Rectangular Plate

The all-edge simply supported rectangular plate as shown in Fig. 2 is considered. The temperature distribution of the plate varies linearly along the thickness. The exact solution of the deflection in z-direction (w) is [13],

$$w(x,y) = \frac{4\alpha\Delta T(1+v)a^2}{\pi^3 t}\sum_{m=1,3,5}^{\infty}\frac{1}{m^3}\sin\frac{m\pi x}{a}\left[1 - \frac{\cosh\left(\dfrac{m\pi y}{a}\right)}{\cosh\left(\dfrac{m\pi b}{2a}\right)}\right] \qquad (30)$$

The geometric properties of plates are the width (a) of 4 m, the length (b) of 2 m, and the thickness (t) of 0.01 m.

The physical properties of the plate are consisted of the thermal expansion coefficient (α) of 2.3×10^{-7} /°C, the Poisson's ratio (v) of 0.33, and the modulus of elasticity (E) of 72 GPa. The temperatures of the upper surface (T_U) of the plate are set to be 100 °C and the lower surface (T_L) of the plate are set to be 25 °C.
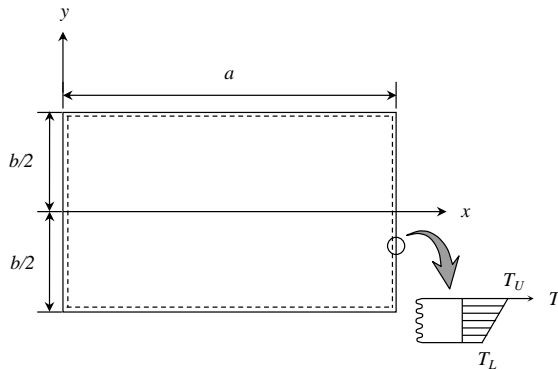

Fig. 2. All-edge simply supported rectangular plate with linear temperature distribution along the thickness.

Due to its symmetry, only the top right quarter of the plate in Fig. 2 was modeled and analyzed. The finite element models with the uniform mesh size of 8×4, 16×8 and 20x10 intervals (45, 153 and 231 nodes, respectively) as shown in Fig. 3(a)-(c) were used in this analysis. Three element types, GCT, DKT and BCIZ, were used in the analysis. From the problem statement, the plate tended to bend with the maximum transverse deflections occurred at the center of the plate. The maximum transverse deflections at the center of the plate obtained from using all elements were shown in Fig. 4. The results from all element types converge to the exact solution as the mesh size decreased. It was obvious that the results obtained from the proposed GCT element and DKT element provided high solution accuracy as they closely matched the exact solution while the solutions obtained from the non-conforming BCIZ element were not as accurate as the others.
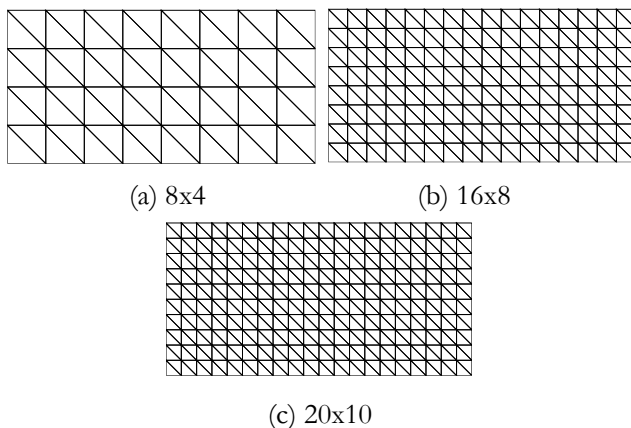

(a) 8x4   (b) 16x8

(c) 20x10

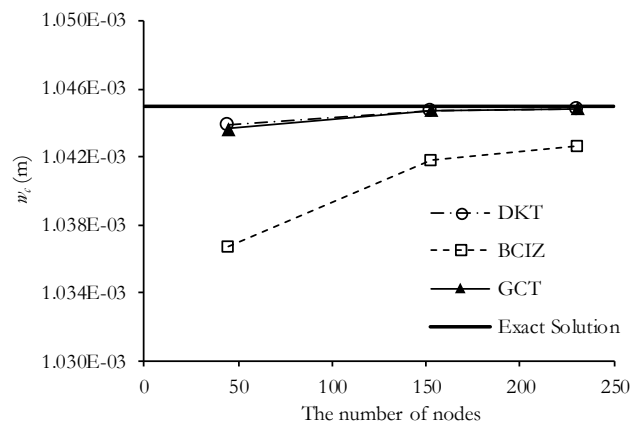Fig. 3. Finite element meshes in the computations.

Fig. 4. Deflections at the center of the plate (w_c) with mesh refinement.

4.2. Clamped and Simply Supported Plate

The rectangular plate of which the sides are clamped and simply supported is considered. The temperature distribution of the plate varies linearly along the thickness. This plate is clamped along the edges $y = b/2$ and $y = -b/2$ of the plate, and the plate is simply supported along the edges $x = 0$ and $x = a$ of the plate as shown in Fig. 5. The exact solution of the deflection (w) is given as [14],

$$w(x,y) = \sum_{m=1,3,5}^{\infty} \left(A_m \cosh \alpha_m y + D_m y \sinh \alpha_m y + K_m \right) \sin \alpha_m x \quad (31)$$

where α_m, A_m, D_m, K_m and Δ_m are,

$$\alpha_m = \frac{m\pi}{a} \quad (32)$$

$$A_m = -K_m \left(\frac{1}{2} \alpha_m b \cosh \frac{1}{2} \alpha_m b + \sinh \frac{1}{2} \alpha_m b \right) / \Delta_m \quad (33)$$

$$D_m = K_m \alpha_m \left(\sinh \frac{1}{2} \alpha_m b \right) / \Delta_m \quad (34)$$

$$K_m = \frac{4M_T}{aD\alpha_m^3} \quad (35)$$

$$\Delta_m = \frac{1}{2} \alpha_m b + \sinh \frac{1}{2} \alpha_m b \cosh \frac{1}{2} \alpha_m b \quad (36)$$

while D and M_T are given in Eq. (2) and Eq. (3), respectively.

The dimension of plate is the width (a) of 2 m and the length (b) of 4 m. The thickness of the plate (t) is 0.01 m. The modulus of elasticity (E) of the plate is defined as 190 GPa. The Poisson's ratio (v) and the thermal expansion coefficient (α) of the plate are 0.3 and 16×10^{-6} /°C, respectively. The temperatures of the upper surface (T_U) of the plate is 60 °C, and temperatures of the lower surface (T_L) of the plate is 0 °C.
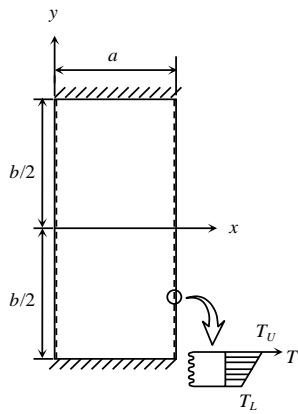
Fig. 5. Clamped and simply supported rectangular plate with linear temperature distribution along the thickness.

Due to the symmetry of the problem, an upper right quarter of the plate was used in this analysis. The finite element models consisted of the uniform mesh size of 4x8, 8x16 and 16x32 mesh intervals with 45 nodes, 153 nodes and 561 nodes, respectively. The example of 4x8 finite element model using in the analysis was shown in Fig. 6. The maximum transverse deflections at the center of the plate (w_c) obtained in the present analysis were shown in Fig. 7. It can be observed that the results obtained from all element types converge to the exact solution as the mesh sizes were decreased. The results showed that the GCT element performed very well and provided higher solution accuracy than other element types.
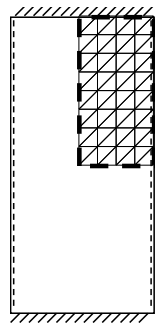

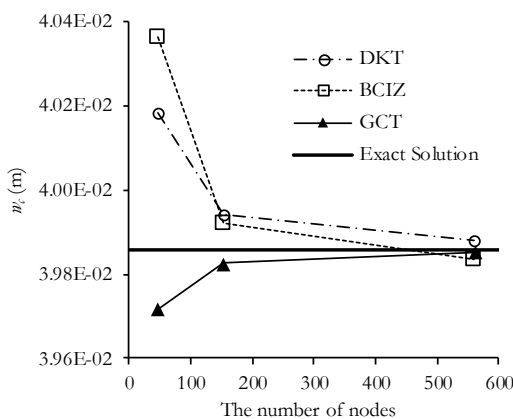Fig. 6. The example of 4x8 finite element model using in the analysis.

Fig. 7. Deflections at the center of the plate (w_c) with mesh refinement.

4.3. Parallelogram Plate

The simply supported parallelogram plate with the linear temperature distribution through the plate thickness shown in Fig. 8 is considered. The plate geometry properties in this analysis are $a = 2$ m, $b = 1$ m, $\gamma = 30°$ and the thickness (t) = 0.01 m. The modulus of elasticity (E) of the plate is 190 GPa. The Poisson's ratio (v) and the thermal expansion coefficient (α) of the plate are 0.3 and 16×10^{-6} /°C, respectively. The plate has the upper surface temperature (T_U) = 60 °C and the lower surface temperature (T_L) = 0 °C. The exact solution of the central transverse deflection (w_c) is given by [15],

$$w_c = 0.090135 \frac{M_T \, b^2}{D} \qquad (37)$$

where D and M_T are given in Eq. (2) and Eq. (3), respectively.
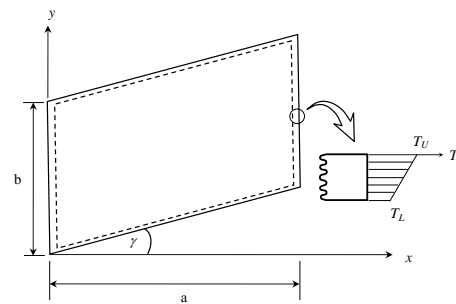

Fig. 8. Simply supported parallelogram plate with linear temperature distribution along the thickness.

The finite element model was discretized into uniform meshes of 8x4 (45 nodes), 16x8 (153 nodes) and 20x10 (231 nodes) intervals as shown in Figs. 9(a)-(c). The central transverse deflections obtained from each element type were compared with the exact solution and shown in Fig. 10. The results indicated that both DKT and GCT elements obviously provided good solution accuracy while the solution obtained from the non-conforming BCIZ element diverged from the exact solution.
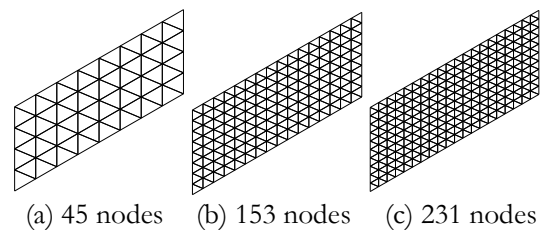

(a) 45 nodes   (b) 153 nodes   (c) 231 nodes

Fig. 9. Finite element meshes of parallelogram plate.

5. Conclusion

The generalized conforming triangular (GCT) element for thermal bending analysis of thin plate caused by the temperature difference along the plate thickness was presented. The derived closed-form expressions of

the GCT element for thermal bending analysis were simple and can be applied in the computer program directly. The presented examples demonstrated that the GCT element with the proposed thermal load finite element formulation provided good solution accuracy. In addition, the results obtained from the proposed element also converged to the exact solution with the meshes refinement. The solution accuracy obtained from both DKT and GCT elements were quite in the same high quality; however, the generalized conforming element was better when we considered in the simplicity of its formulation. Moreover, the non-conforming BCIZ element was somehow unreliable in some cases as we could see in the third example that it provided diverged solution.
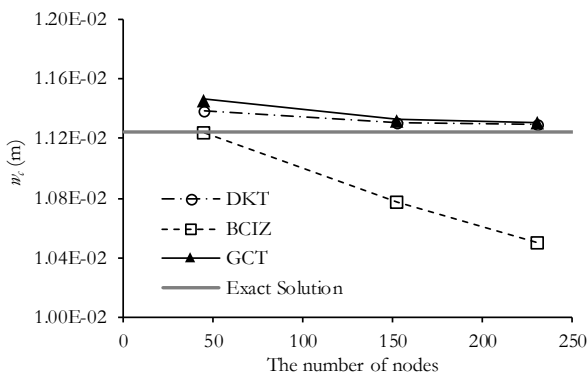

Fig. 10 Deflections at the center of the plate (w_c) with mesh refinement.

References

[1] M. M. Hrabok and T. M. Hrudey, "A review and catalogue of plate bending finite elements," *Comput. Struct.*, vol. 19, no. 3, pp. 479-495, 1984.

[2] J. Mackerle, "Static and dynamic analysis of plates using finite element and boundary elements - A bibliography (1992-1994) ," *Finite Elem. Anal. Des.*, vol. 20, no. 2, pp. 139-154, 1995.

[3] J. L. Batoz, K. J. Bathe, and L. W. Ho, "A study of three-node triangular plate bending elements," *Int. J. Numer. Meth. Eng.*, vol. 15, no. 12, pp. 1771-1812, 1980.

[4] J. L. Batoz, C. L. Zheng, and F. Hammadi, "Formulation and evaluation of new triangular, quadrilateral, pentagonal and hexagonal discrete Kirchhoff plate/shell elements," *Int. J. Numer. Meth. Eng.*, vol. 52, no. 5-6, pp. 615-630, 2001.

[5] G. P. Bazeley, Y. K. Cheung, B. M. Irons, and O. C. Zienkiewicz, "Triangular elements in plate bending conforming and non-conforming solution," in *Proceedings 1st Conference on Matrix Methods in Structural Mechanics*, Air Force Ins. Tech., Wright-Patterson A.F. Base, Ohio, United States, 1965, pp. 547-576.

[6] O. C. Zienkiewicz and R. L. Taylor, *The Finite Element Method for Solid and Structural Mechanics*, 6th ed. Oxford, United Kingdom: Butterworth-Heinemann, 2005.

[7] P. Bhothikhun and P. Dechaumphai, "Adaptive DKT finite element for plate bending analysis of built-up structures," *IJMME*, vol. 14, no. 1 pp. 12-20, 2014.

[8] P. Bhothikhun and P. Dechaumphai, "Development of DKT finite element formulation for thermal bending of thin plate," *J. Therm. Stresses.*, vol. 38, no. 7, pp. 775-791, 2015.

[9] L. Zhifei, "Generalized conforming triangular elements for plate bending," *Commun. Numer. Meth. En.*, vol. 9, no. 1, pp. 53-65, Jan. 1993.

[10] L. Yuqiu, B. Xiaoming, L. Zhifei, and X. Yin, "Generalized conforming plate bending elements using point and line compatibility conditions," *Comput. Struct.*, vol. 54, no. 4, pp. 717-723, 1995.

[11] P. Dechaumphai, *Finite Element Method: Fundamentals and Applications*. Oxford, United Kingdom: Alpha Science International, 2010.

[12] L. Yuqiu and X. Kegui, "The generalized conforming element," *China Civil Engineering Journal*, vol. 20, no. 1, pp. 1-14, 1987.

[13] B. A. Boley and J. H. Weiner, *Theory of Thermal Stresses*, New York: Dover Publications, 1997.

[14] R. B. Hetnarski, *Encyclopedia of Thermal Stresses*, New York: Springer, 2014.

[15] V. M. Kulakov, A. A. Uspenskii, and A. N. Frolov, "Thermal Deflection in a Parallelogram Plate," *Strength. Mater.*, vol. 7, no. 11, pp. 1362-1364, 1975.

Appendix

The closed form of the stiffness matrix $[K]$ given in Eq. (25) is,

$$[K] = [R]^T [Q][R] \qquad (A1)$$

where the matrices $[R]$ and $[Q]$ is defined by,

$$[R] = [C][A] \qquad (A2)$$

$$[C] = -\frac{1}{4A^2}\begin{bmatrix}
2b_1b_2 & 2b_2b_3 & 2b_3b_1 & 3b_1{}^2 & -3b_2{}^2 & -3b_3{}^2 \\
2b_1b_2 & 2b_2b_3 & 2b_3b_1 & -3b_1{}^2 & 3b_2{}^2 & -3b_3{}^2 \\
2b_1b_2 & 2b_2b_3 & 2b_3b_1 & -3b_1{}^2 & -3b_2{}^2 & 3b_3{}^2 \\
2c_1c_2 & 2c_2c_3 & 2c_3c_1 & 3c_1{}^2 & -3c_2{}^2 & -3c_3{}^2 \\
2c_1c_2 & 2c_2c_3 & 2c_3c_1 & -3c_1{}^2 & 3c_2{}^2 & -3c_3{}^2 \\
2c_1c_2 & 2c_2c_3 & 2c_3c_1 & -3c_1{}^2 & -3c_2{}^2 & 3c_3{}^2 \\
2(b_1c_2+b_2c_1) & 2(b_2c_3+b_3c_2) & 2(b_3c_1+b_1c_3) & 6b_1c_1 & -6b_2c_2 & -6b_3c_3 \\
2(b_1c_2+b_2c_1) & 2(b_2c_3+b_3c_2) & 2(b_3c_1+b_1c_3) & -6b_1c_1 & 6b_2c_2 & -6b_3c_3 \\
2(b_1c_2+b_2c_1) & 2(b_2c_3+b_3c_2) & 2(b_3c_1+b_1c_3) & -6b_1c_1 & -6b_2c_2 & 6b_3c_3
\end{bmatrix}$$

$$(A3)$$

$$[A] = \begin{bmatrix}
0 & -\frac{1}{2}b_3 & -\frac{1}{2}c_3 & 0 & \frac{1}{2}b_3 & \frac{1}{2}c_3 & 0 & 0 & 0 \\
0 & 0 & 0 & 0 & -\frac{1}{2}b_1 & -\frac{1}{2}c_1 & 0 & \frac{1}{2}b_1 & \frac{1}{2}c_1 \\
0 & \frac{1}{2}b_2 & \frac{1}{2}c_2 & 0 & 0 & 0 & 0 & -\frac{1}{2}b_2 & -\frac{1}{2}c_2 \\
-2 & -\frac{1}{2}(b_2-b_3) & -\frac{1}{2}(c_2-c_3) & 1+r_1 & -\frac{1}{2}(r_1b_1-b_3) & -\frac{1}{2}(r_1c_1-c_3) & 1-r_1 & -\frac{1}{2}(r_1b_1+b_2) & -\frac{1}{2}(r_1c_1+c_2) \\
1-r_2 & -\frac{1}{2}(r_2b_2+b_3) & -\frac{1}{2}(r_2c_2+c_3) & -2 & -\frac{1}{2}(b_3-b_1) & -\frac{1}{2}(c_3-c_1) & 1+r_2 & -\frac{1}{2}(r_2b_2-b_1) & -\frac{1}{2}(r_2c_2-c_1) \\
1+r_3 & -\frac{1}{2}(r_3b_3-b_2) & -\frac{1}{2}(r_3c_3-c_2) & 1-r_3 & -\frac{1}{2}(r_3b_3+b_1) & -\frac{1}{2}(r_3c_3+c_1) & -2 & -\frac{1}{2}(b_1-b_2) & -\frac{1}{2}(c_1-c_2)
\end{bmatrix}$$

$$(A4)$$

$$[Q] = \frac{Et^3}{12(1-v^2)}\begin{bmatrix} [P] & v[P] & [0] \\ v[P] & [P] & [0] \\ [0] & [0] & \frac{1-v}{2}[P] \end{bmatrix} \quad (A5)$$

$$[P] = \frac{A}{12}\begin{bmatrix} 2 & 1 & 1 \\ 1 & 2 & 1 \\ 1 & 1 & 2 \end{bmatrix} \quad (A6)$$

The vector of the nodal forces due to the thermal load $\{F_T\}$ given in Eq. (29) is,

$$\{F_T\} = \frac{1}{1-v}M_T[BA]\begin{Bmatrix} 1 \\ 1 \\ 0 \end{Bmatrix} \quad (A7)$$

where the closed form of $[BA]$ is in the form of,

$$[BA] = [A]^T[T] \quad (A8)$$

$$[T] = \frac{1}{4A}\begin{bmatrix} -2b_1b_2 & -2c_1c_2 & -2(b_1c_2+b_2c_1) \\ -2b_2b_3 & -2c_2c_3 & -2(b_2c_3+b_3c_2) \\ -2b_3b_1 & -2c_3c_1 & -2(b_3c_1+b_1c_3) \\ b_1^2 & c_1^2 & 2b_1c_1 \\ b_2^2 & c_2^2 & 2b_2c_2 \\ b_3^2 & c_3^2 & 2b_3c_3 \end{bmatrix} \quad (A9)$$

Chatthanon Bhothikhun was born in Bangkok, Thailand in 1983. He received the B.Eng., M.Eng. and Ph.D. degrees in mechanical engineering from Chulalongkorn University, Bangkok, Thailand, in 2005, 2010 and 2015, respectively.

From 2008 to 2015, he was a Research Assistant at Center of Excellence in Computational Mechanism (CMRL), Department of Mechanical Engineering, Chulalongkorn University. Since 2016, he has been a Lecturer with the Mechanical Engineering Department, Silpakorn University, Nakhon Pathom, Thailand. His research interests include Finite Element in Plate Bending Analysis, Numerical Method in Engineering and Computational Fluid Dynammics in Fluidized-bed Combustor.

Dr. Bhothikhun was a recipient of the International Conference on Science, Technology and Innovation for Sustainable Well-Being (STISWB) Best Paper Award in 2016 and 2018, and the Thai Society of Mechanical Engineers International Conference on Mechanical Engineering (TSME-ICoME) Best Paper Runner-up Awards in 2016.